Journal of Cellular Biochemistry 24:207–216 (1984)
Protein Transport and Secretion 205–214

A Model for the Structure of Fumarate Reductase in the Cytoplasmic Membrane of Escherichia coli

Joel H. Weiner, Bernard D. Lemire, Robert W. Jones, Wayne F. Anderson, and Douglas G. Scraba

Department of Biochemistry (J.H.W., B.D.L., R.W.J., D.G.S.) and MRC Group on Protein Structure and Function (W.F.A.), University of Alberta, Edmonton, Alberta, Canada T6G 2H7

By a recombinant DNA approach we have prepared *Escherichia coli* cytoplasmic membranes that are highly enriched in the terminal electron transfer enzyme fumarate reductase. This enzyme is composed of four nonidentical subunits in equal molar ratio. A 69,000-dalton covalent flavin-containing subunit and a 27,000-dalton nonheme iron-containing subunit make up a membrane extrinsic catalytic domain. Two very hydrophobic subunits of 15,000 and 13,000 daltons make up the hydrophobic membrane anchor domain. Electron microscopy of negatively stained membranes shows a characteristic knob-and-stalk-type structure composed of the catalytic domain. The anchor polypeptides have been analyzed for hydrophobic segments and α-helical content and a model for their organization within the lipid bilayer is presented. The results reviewed in this paper suggest a model for the fumarate reductase complex in the cytoplasmic membrane

Key words: alpha-helical analysis, fumarate reductase, membrane protein structure

Anaerobic growth of Escherichia coli on medium containing glycerol (or glycerol-3-phosphate) plus fumarate results in the induction of a very simple electron transport chain that conserves the redox energy of electron flow from glycerol-3-phosphate to fumarate as a proton motive force across the membrane [1]. The membrane-associated electron transport chain is composed of only three proteins: an anaerobic glycerol-3-phosphate dehydrogenase, a b-type cytochrome, and fumarate reductase [2]. Recently, a combination of genetic, physical, enzymatic, and electron microscopic studies have converged to suggest a model for the structure of the terminal electron transfer enzyme of this pathway, fumarate reductase, which may be relevant to mitochondrial succinate dehydrogenase and to other membrane-associated iron-flavo-enzyme complexes.

In this paper we propose to review the data relevant to the structure of fumarate reductase and to propose a model for the enzyme complex within the cytoplasmic membrane.

Received May 20, 1983; revised and accepted November 30, 1983.

RESULTS AND DISCUSSION

Genetic Approaches

The fumarate reductase operon is located at 93.5 min on the circular E coli map [3]. Mutants in the structural genes have been isolated [4,5] and complementation approaches have been used with these mutants to identify a plasmid from the Clarke and Carbon colony bank [6], or from a λ phage-E coli bank [7], carrying the fumarate reductase operon. The fumarate reductase operon lies on a 4.4-kilobase (Kb) Hind III fragment of E coli DNA and the entire DNA sequence, and thus inferred amino acid sequence, of this fragment has been determined, primarily by S.T. Cole [8–10]. The fragment codes for four polypeptides of 69,000, 27,000, 15,000, and 13,000 daltons, which are now termed the *frdA*, *frdB*, *frdC*, and *frdD* polypeptides, respectively. Cloning of the Hind III fragment into the multicopy vector pBR322 results in a 20-fold amplification of membrane-associated fumarate reductase activity in strains harboring this plasmid under inducing conditions [11]. We have taken advantage of these highly enriched membranes to study the enzyme in its native environment and as a starting material for enzyme isolation.

The Membrane Extrinsic Domain

Our initial isolation of fumarate reductase indicated that the catalytic activity was associated with an $\alpha\beta$-dimer composed of 69,000- and 27,000-dalton subunits [12]. This form of the enzyme can be readily isolated in a nearly homogeneous form from normal or amplified membrane fractions of anaerobically grown cells by Triton X-100 solubilization and hydrophobic exchange chromatography on a phenyl Sepharose column in the presence of cholate [12]. The isolated detergent-depleted dimer has been extensively characterized by physical and enzymatic techniques [13]. Most relevant to this discussion was the finding that the enzyme bound only 0.15 g of Triton X-100 per g of protein, placing it at the lower limit of membrane-bound proteins [14]. This was unexpected in light of the finding that the enzyme could not be readily removed from the membrane by high or low salt washes, 0.2 M EDTA, or other procedures known to elute extrinsic proteins [12]. Release required complete disruption of the membrane by nonionic detergent. An additional unexpected property was the finding that the purified dimer required anions for activity and optimal thermal and alkaline stability, unlike the membrane-bound activity [15]. As will be shown below this latter property results from removal of the 15,000- and 13,000-dalton membrane-anchor subunits. The 69,000 dalton subunit contains an 8α N-3 histidyl flavin adenine dinucleotide cofactor (FAD, covalently linked to a histidine residue in the polypeptide chain) [16]. Sequence studies of the 69,000-dalton subunit carried out by Cole resulted in identification of a histidine-containing peptide of identical sequence to the covalent flavin binding domain reported by Singer and Kearney [17] some years earlier for beef heart mitochondrial succinate dehydrogenase. It is presumed that the flavin plays an essential role in electron transfer within fumarate reductase, as it does in succinate dehydrogenase [17].

Examination of the sequence of the 69,000-dalton subunit by a Kyte-Doolittle type of analysis [18] for stretches of hydrophobic amino acids, which might serve as a membrane-binding domain, failed to identify any region of significant hydrophobic character (data not shown).

The 27,000-dalton subunit appears to be the iron-sulfur-containing polypeptide. The catalytic dimer (69,000- and 27,000-dalton subunits) has been shown to contain four acid-labile sulfur atoms and four nonheme iron atoms per dimer [9]. The sequence of the 27,000-dalton subunit has an unusual clustering of four cysteine residues with striking homology to the iron-sulfur binding domain of Peptococcus aerogenes ferrodoxin [9], and we presume that this is the iron-sulfur binding site. Although not yet conclusively shown, it appears that a single center of the Fe_4S_4 type is present in the enzyme.

As with the 69,000-dalton subunit, an examination of the hydrophobicity of the 27,000-dalton subunit failed to identify any potential membrane binding domains.

The Membrane Intrinsic Domain

When DNA sequence analysis of the *frd* region of the E coli chromosome was carried out, it became clear that two open reading frames corresponding to polypeptides of 15,000 and 13,000 daltons were located downstream from the *frdB* gene [10]. Recently, we showed that these open reading frames code for components of a fumarate reductase complex [11]. Two small polypeptides of the expected molecular weights could be visualized by Coomassie blue staining of 10–25% sodium dodecyl sulfate-polyacrylamide gradient gels of membranes containing amplified levels of fumarate reductase. We showed that the 15,000- and 13,000-dalton polypeptides were synthesized upon induction of the *frd* operon, were amplified coordinately with the *frdA* and *frdB* polypeptides, and were present in 1:1 mole ratio with the *frdA* and *frdB* polypeptides [11]. Most importantly, a holoenzyme containing equimolar amounts of each subunit was solubilized from the membrane by Triton X-100, treatment and the holoenzyme could be purified by sucrose gradient sedimentation [11]. In our earlier studies of the enzyme we failed to detect the two small polypeptides because their extremely hydrophobic composition caused them to bind very tightly to the phenyl Sepharose column. Apparently when we eluted the reductase activity from the column, it eluted not from the resin, but from the hydrophobic polypeptides. These two hydrophobic polypeptides could be recovered from the column by washing with 1% Triton X-100 [11].

The functional role of the two small polypeptides is at least twofold. First, they serve as anchor polypeptides for the catalytic dimer. We have shown this in two ways. In one approach, a recombinant plasmid, pFRD117, was constructed that carried only the 69,000- and 27,000-dalton sequences in the vector pBR322 [11]. Strains harboring this plasmid and induced by anaerobic growth on fumarate produced very high levels of fumarate reductase, but all the activity was in the soluble cytoplasmic fraction. This activity behaved as a typical soluble protein and could be purified by conventional techniques without resorting to detergents. In a different approach we prepared inverted membrane vesicles by French press lysis of an induced strain harboring a plasmid carrying the entire operon. When such vesicles were washed with 6 M urea, the 69,000- and 27,000-dalton subunits were removed; however, the two hydrophobic polypeptides remained membrane-associated. These "urea-stripped" vesicles can specifically bind fresh catalytic dimers in a saturable fashion.

The second function of the hydrophobic polypeptides is to modulate the activity and stability of the catalytic dimer. The catalytically active dimer requires anions for activity and stability whereas the holoenzyme (tetramer), or the membrane-bound activity does not [11,15].

TABLE I. Amino Acid Similarities*

	ALA (A)	ARG (R)	ASN (N)	ASP (D)	CYS (C)	GLN (Q)	GLU (E)	GLY (G)	HIS (H)	ILE (I)
ALA	1.00	−0.11	−0.25	−0.25	0.21	−0.09	0.10	−0.07	0.17	−0.20
ARG	−0.11	1.00	0.19	−0.01	−0.29	0.28	0.12	−0.36	0.56	−0.67
ASN	−0.25	0.19	1.00	0.31	−0.35	0.48	0.11	−0.15	0.04	−0.98
ASP	−0.25	−0.01	0.31	1.00	−0.51	0.12	0.29	−0.12	−0.15	−1.12
CYS	0.21	−0.29	−0.35	−0.51	1.00	−0.20	−0.10	−0.28	−0.04	−0.02
GLN	−0.09	0.28	0.48	0.12	−0.20	1.00	0.34	−0.42	0.30	−0.83
GLU	0.10	0.12	0.11	0.29	−0.10	0.34	1.00	−0.34	0.24	−0.69
GLY	−0.07	−0.36	−0.15	−0.12	−0.28	−0.42	−0.34	1.00	−0.39	−0.70
HIS	0.17	0.56	0.04	−0.15	−0.04	0.30	0.24	−0.39	1.00	−0.35
ILE	−0.20	−0.67	−0.98	−1.12	−0.02	−0.83	−0.69	−0.70	−0.35	1.00
LEU	0.21	−0.45	−0.71	−0.81	0.38	−0.49	−0.31	−0.52	−0.10	0.38
LYS	0.02	0.61	0.23	0.13	−0.28	0.34	0.24	−0.28	0.43	−0.80
MET	0.23	−0.24	−0.46	−0.64	0.41	−0.14	−0.06	−0.58	0.14	0.09
PHE	0.12	−0.15	−0.52	−0.65	0.11	−0.33	−0.20	−0.47	0.18	0.36
PRO	−0.49	−0.48	−0.17	−0.03	−0.72	−0.53	−0.50	0.34	−0.64	−1.23
SER	−0.01	0.15	0.50	0.31	−0.29	0.20	0.07	0.23	0.07	−0.78
THR	0.09	0.29	0.34	0.11	−0.19	0.22	0.09	0.04	0.31	−0.53
TRP	−0.12	−0.02	−0.33	−0.53	0.07	−0.17	−0.14	−0.50	0.18	−0.01
TYR	−0.12	0.08	−0.13	−0.36	−0.04	−0.14	−0.16	−0.19	0.18	−0.09
VAL	−0.21	−0.70	−0.98	−1.13	−0.02	−0.85	−0.72	−0.66	−0.39	0.86

*1.00 corresponds to perfect similarity.

Secondary-Structure Predictions for the Anchor Polypeptides

The anchor polypeptides have been shown to lack cleaved leader sequences [10], thus the inferred amino acid sequences obtained from DNA sequence analysis correspond to the functional proteins. We have examined these sequences for relative hydrophobicity and hydrophilicity according to the method of Kyte and Doolittle [18]. As can be seen in Figure 1, each of the anchor polypeptides has three relatively long stretches of hydrophobic amino acids separated by relatively short stretches of charged and polar residues. By analogy to other membrane-bound proteins [20], it seemed likely that the hydrophobic stretches were in an α-helical configuration. To further test this idea the *frdC* and *frdD* amino acid sequences were compared with each other and with the amino acid sequence of bacteriorhodopsin [20]. The procedure used will be reported elsewhere (Anderson, in preparation). Briefly, the comparison of the sequences is by the method of Fitch [21] except that the scores relating individual amino acids were assigned on the basis of the structural similarities of the amino acids. Structural similarities are used rather than the genetic code [21] or observed amino acid substitutions in homologous sequences [22] because the aim is to detect regions which potentially have similar structures and are not necessarily related through divergent evolution. The score for replacing one amino acid with another is derived from the difference between the two amino acids in terms of hydrophobicity [18,23], secondary structure preferences [23], polarity, and size. The scores used for the replacement of any amino acid by any other are given in Table I. This table of individual scores is used to calculate the score for each span of residues for every alignment and the matrix of scores obtained is then displayed as in Figures 2 and 4. When this analysis was carried out on the *frdC* polypeptide versus bacteriorhodopsin the matrix (Fig. 2) does not show the strong diagonal features that occur with homologous amino acid sequences, but rather they indicate regions of the sequences

LEU (L)	LYS (K)	MET (M)	PHE (F)	PRO (P)	SER (S)	THR (T)	TRP (W)	TYR (Y)	VAL (V)
0.21	0.02	0.23	0.12	−0.49	−0.01	0.09	−0.12	−0.12	−0.21
−0.45	0.61	−0.24	−0.15	−0.48	0.15	0.29	−0.02	0.08	−0.70
−0.71	0.23	−0.46	−0.52	−0.17	0.50	0.34	−0.33	−0.13	−0.98
−0.81	0.13	−0.64	−0.65	−0.03	0.31	0.11	−0.53	−0.36	−1.13
0.38	−0.28	0.41	0.11	−0.72	−0.29	−0.19	0.07	−0.04	−0.02
−0.49	0.34	−0.14	−0.33	−0.53	0.20	0.22	−0.17	−0.14	−0.85
−0.31	0.24	−0.06	−0.20	−0.50	0.07	0.09	−0.14	−0.16	−0.72
−0.52	−0.28	−0.58	−0.47	0.34	0.23	0.04	−0.50	−0.19	−0.66
−0.10	0.43	0.14	0.18	−0.64	0.07	0.31	0.18	0.18	−0.39
0.38	−0.80	0.09	0.36	−1.23	−0.78	−0.53	−0.01	−0.09	0.86
1.00	−0.47	0.51	0.43	−0.98	−0.57	−0.39	0.13	−0.09	0.31
−0.47	1.00	−0.25	−0.30	−0.37	0.21	0.21	−0.22	−0.16	−0.82
0.51	−0.25	1.00	0.34	−1.01	−0.42	−0.23	0.18	−0.07	0.03
0.43	−0.30	0.34	1.00	−0.88	−0.37	−0.10	0.48	0.32	0.29
−0.98	−0.37	−1.01	−0.88	1.00	0.07	−0.23	−0.78	−0.50	−1.21
−0.57	0.21	−0.42	−0.37	0.07	1.00	0.61	−0.33	−0.02	−0.77
−0.39	0.21	−0.23	−0.10	−0.23	0.61	1.00	−0.11	0.20	−0.51
0.13	−0.22	0.18	0.48	−0.78	−0.33	−0.11	1.00	0.50	−0.08
−0.09	−0.16	−0.07	0.32	−0.50	−0.02	0.20	0.50	1.00	−0.11
0.31	−0.82	0.03	0.29	−1.21	−0.77	−0.51	−0.08	−0.11	1.00

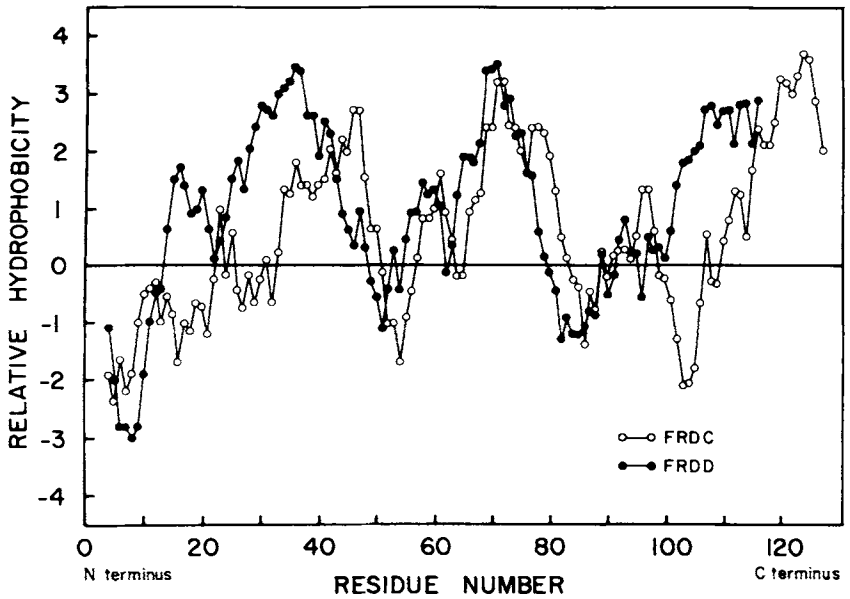

Fig. 1. Plot of hydrophobicity versus position in the amino acid sequence for *frdC* (○—○) and *frdD* (●—●). The hydrophobicity values are averages of the Kyte-Doolittle parameters [18] over four consecutive residues.

with similar structural preferences (the darker patches indicated by the arrows on the abcissa of Fig. 2). Similar results were obtained when the *frdD* protein was compared with bacteriorhodopsin. The regions of similarity correspond to segments of the bacteriorhodopsin structure known to be α-helical [20] and to be embedded in the lipid bilayer. It thus seems likely that the anchor polypeptides of fumarate reductase have similar structural features and are embedded in the bilayer. The length of the

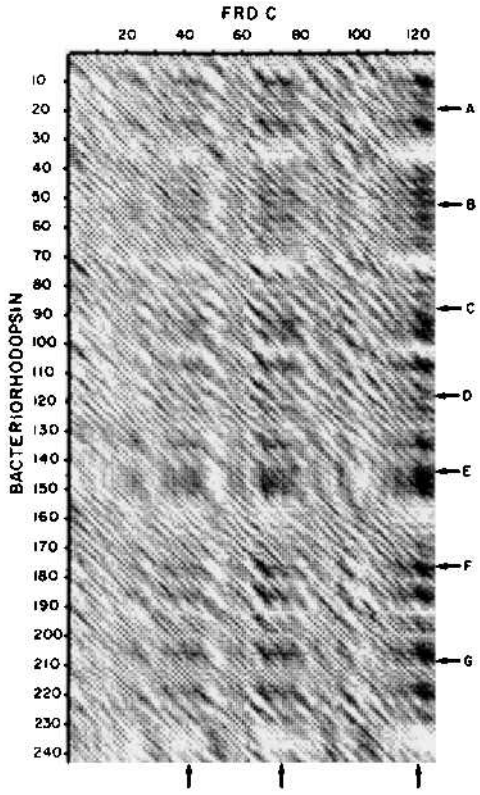

Fig. 2. Matrix relating the degree of similarity of the bacteriorhodopsin and the *frdC* amino acid sequences. Each point in the matrix is the result of the comparison of a ten-residue segment of bacteriorhodopsin with a ten-residue segment of *frdC*. The scores of all possible ten-residue comparisons are fit by a standard Gaussian distribution, and the matrix is plotted such that the better the score (in standard deviations from the mean), the larger the black dot. The positions of the proposed seven transmembrane α-helices in bacteriorhodopsin [20] are indicated by the arrows A–G. The regions of the *frdC* polypeptide indicated by arrows are the proposed transmembrane α-helices.

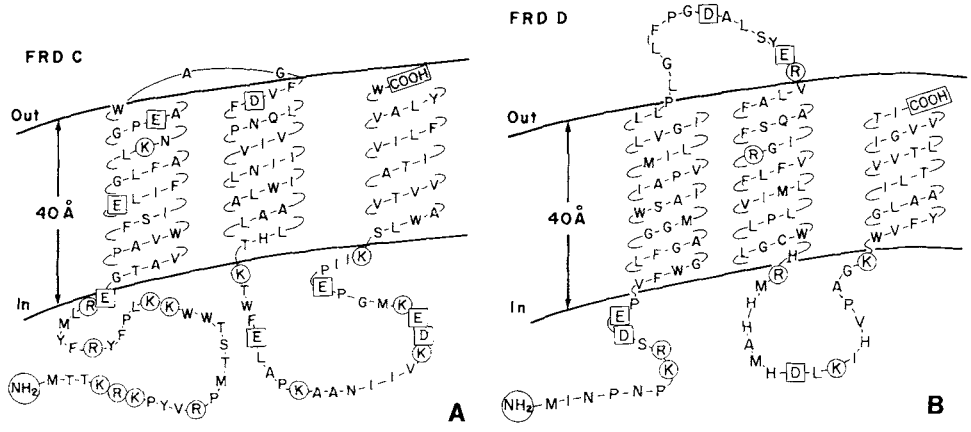

Fig. 3. A model for the organization of the *frdC* protein A) and the *frdD* protein B) with respect to the lipid bilayer. Amino acids with positively charged side chains are shown as circles and amino acids with negatively charged side chains are shown as squares.

hydrophobic segments correspond to lengths of about 24 ± 4 amino acid residues; such a stretch of polypeptide would be long enough to traverse the hydrophobic core of a lipid bilayer of 40 Å. Secondary structure calculations also predict reverse turns in the nonhydrophobic segments. In Figure 3A,B we propose a model for the secondary structure of the *frdC* and *frdD* polypeptides within the lipid bilayer that incorporates these predictions. Each polypeptide weaves through the membrane three times, and although they bear little sequence homology, they are strikingly similar in overall structure when analyzed by the comparative approach described above (Fig. 4). In this model very few charges are buried within the lipid bilayer. The *frdC* protein has a lysine and glutamate between residues 51 and 55, which will make a salt bridge. A lone glutamate is found in the *frdC* hydrophobic domain and a lone arginine in the bilayer spanning portions of the *frdD* protein. These residues may have important functional roles. Several of the helices have proline residues that will probably introduce bends of approximately 20° in the helices, but may not prevent the overall helical conformation.

The overall orientation of the protein is unknown; however, the orientation shown in Figure 3 seems most likely, as it provides segments of the anchor polypeptides to interact with the catalytic subunits which are known to be on the cytoplasmic surface and aligns the polypeptide with the membrane potential (internal negative). Topology studies of the anchor polypeptides to be reported elsewhere (Lemire and Weiner, in preparation) substantiate this model. This structure also suggests a mechanism for anchor assembly within the bilayer. The positive charges at the N-terminal

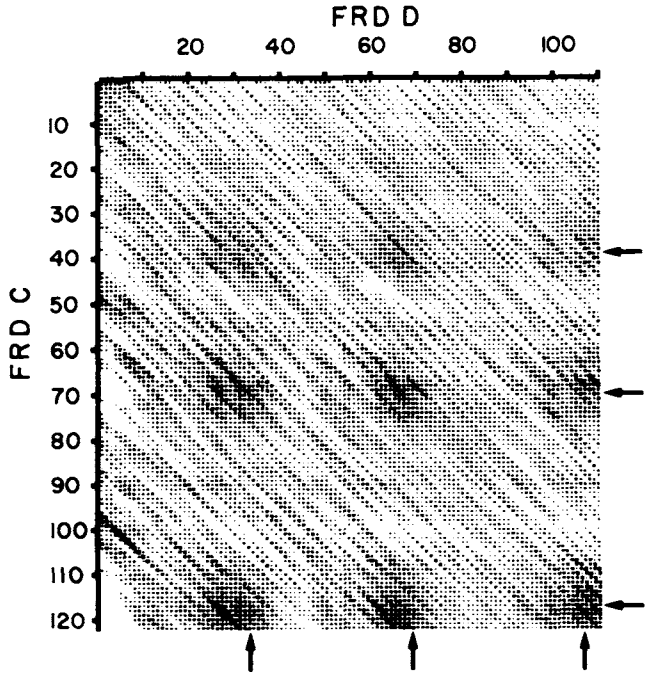

Fig. 4. Similarity matrix (as in Fig. 2) of the *frdC* and *frdD* polypeptides. Note that the regions of higher than average similarity, indicated by the arrows, correspond to those regions of *frdC* that also were most similar to the transmembrane α-helices of bacteriorhodopsin and that these regions of similarity between *frdC* and *frdD* coincide with the hydrophobic segments of the polypeptides (Fig. 2).

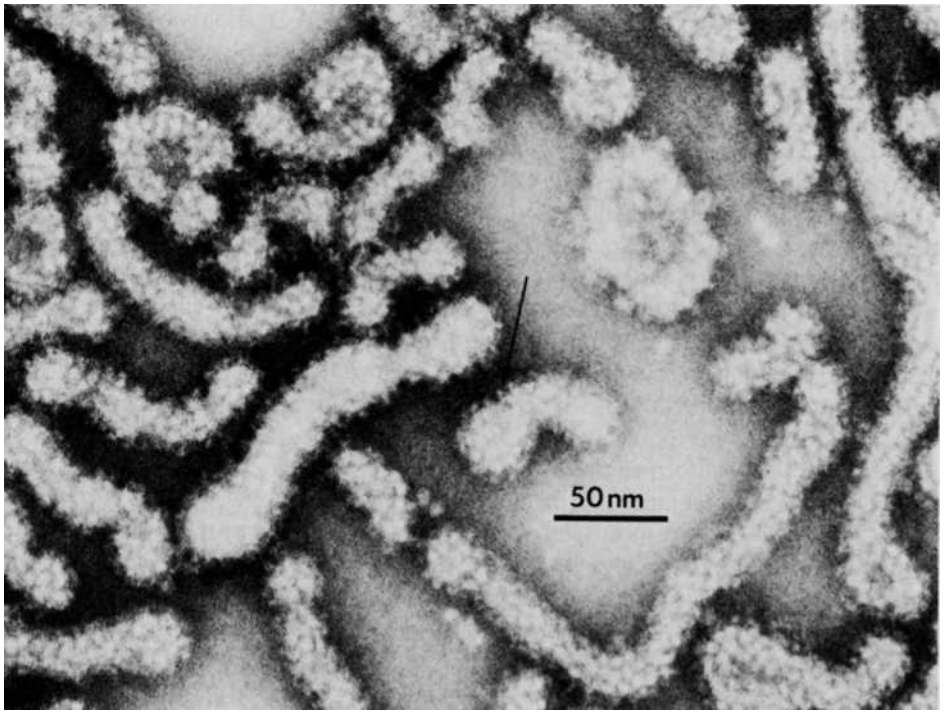

Fig. 5. Electron micrograph of inner membrane vesicles prepared by French press lysis of anaerobically grown E coli HB101 carrying a plasmid with the frd operon [11].

may allow the growing polypeptide to bind to the membrane by ionic interaction in a fashion analogous to that proposed for signal sequences [25]. Subsequently, the first two α-helical segments may enter the membrane as a helical hairpin [26] and the third segment partition into the membrane once polypeptide synthesis is complete and the protein is released from the ribosome.

Electron Microscopic Studies

When negatively stained preparations of the membranes highly enriched in fumarate reductase were examined in the electron microscope, a knob-and-stalk-type structure was observed on the cytoplasmic surface, which correlated with fumarate reductase expression (Fig. 5). We have shown that these extramembranal structures bind antifumarate reductase γ-globulin and can be removed from the membranes by the 6 M urea wash [19]. As described above, the wash contained the 69,000- and 27,000-dalton subunits, whereas the 15,000- and 13,000-dalton subunits remained associated with the membrane. Reconstitution studies have shown that the anchor polypeptides remain functional and can rebind fresh catalytic dimers in a saturable fashion [19].

In addition to the typical inverted membrane vesicles expected in a French pressure cell lysis of bacteria, we observed novel tubular structures covered with a helical arrangement of the knobs and stalks (Fig. 5). These tubules are not an artifact of the lysis procedure and can be observed by thin section electron microscopy in

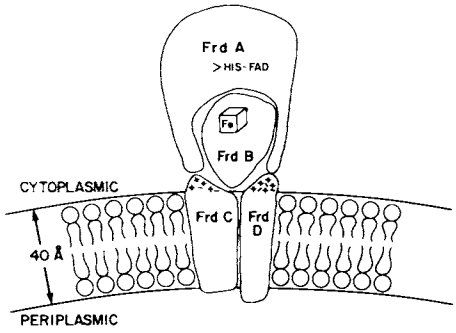

Fig. 6. A model for the fumarate reductase enzyme complex within the lipid bilayer.

intact bacteria with greatly amplified levels of fumarate reductase. The tubules appear to aggregate into bundles which can extend the entire length of the bacterium. The isolation and biochemical characterization of these tubules will be reported elsewhere (J.H. Weiner, B.D. Lemire, M.L. Elmes, R.D. Bradley and D.G. Scraba, J Bacteriol, May 1984).

A Model for the Structure of the Holoenzyme

The information summarized in the preceding sections can be combined to generate the working model for fumarate reductase that is shown in Figure 6. The enzyme is seen to be composed of a membrane extrinsic domain composed of 69,000- and 27,000-dalton subunits forming the stalk and knobs seen in electron micrographs and a membrane intrinsic domain composed of the 15,000- and 13,000-dalton anchor subunits, which we believe to be transmembranal proteins.

We have found that the 27,000-dalton subunit is partially inaccessible to labeling by phenylglyoxal, iodosulfanilic acid, and lactoperoxidase catalyzed iodination (Lemire and Weiner, unpublished results) as well as to chymotrypsin-catalyzed proteolysis [19]. These results lead us to propose that the 69,000-dalton subunit envelopes most of the 27,000-dalton subunit. Further cross-linking studies with dithiobis (succinimidylpropionate) show that the 69,000- and 27,000-dalton subunits interact [13] and that the 15,000-dalton subunit can cross-link to the 69,000-dalton subunit [30], indicating that these two subunits are in close proximity. The 15,000- and 13,000-dalton subunits can be cross-linked by dithiobis (succinimidylpropionate) only from the inside surface, as would be predicted from examination of Figure 3 (all the lysines are on the inside) (Lemire and Weiner, unpublished results). Further studies of subunit interactions and the possible association of other components of the electron transport chain with fumarate reductase are underway.

The organization of this enzyme complex resembles the F_0/F_1 ATPase in having an extrinsic stalk-and-knob structure and a transmembranal domain [27]. In particular, the membrane intrinsic domain resembles remarkably similar domains in bacteriorhodopsin [20], the F_0 portion of ATPase [28] and the lac carrier [29], three proteins known to be involved in proton translocation. The possibility that fumarate reductase acts as a proton pump is presently under investigation.

ACKNOWLEDGMENTS

Work reported in this paper was supported by grants from the Medical Research Council of Canada to J.H.W. and D.G.S. and to the MRC Group on Protein Structure and Function. B.D.L. and R.W.J. were supported by the Alberta Heritage Foundation for Medical Research.

REFERENCES

1. Harold FM: Curr Top Bioenerget 6:83–149, 1976.
2. Haddock BA, Jones CW: Bacteriol Rev 41:47–99, 1977.
3. Bachmann BJ, Low KB: Microbiol Rev 44:1–56, 1980.
4. Spencer ME, Guest JR: J Bacteriol 114:563–570, 1973.
5. Lohmeier E, Hagen DS, Dickie P, Weiner JH: Can J Biochem 59:158–164, 1981.
6. Clarke L, Carbon J: Cell 9:91–99, 1976.
7. Cole ST, Guest JR: Eur J Biochem 102:65–71, 1979.
8. Cole ST: Eur J Biochem 122:479–484, 1982.
9. Cole ST, Grundstrom T, Jaurin B, Robinson JJ, Weiner JH: Eur J Biochem 126:211–216, 1982.
10. Grundstrom T, Jaurin B: Proc Natl Acad Sci USA 79:1111–1115.
11. Lemire BD, Robinson JJ, Weiner JH: J Bacteriol 152:1126–1131, 1982.
12. Dickie P, Weiner, JH: Can J Biochem 57:813–821, 1979.
13. Robinson JJ, Weiner JH: Can J Biochem 60:811–816, 1982.
14. Clarke S: J Biol Chem 250:4007–4021, 1975.
15. Robinson JJ, Weiner JH: Biochem J 199:473–477, 1981.
16. Weiner JH, Dickie P: J Biol Chem 254:8590–8593, 1979.
17. Singer TP, Kearney EB, Kenney WC: Adv Enzymol 37:189–272, 1973.
18. Kyte J, Doolittle RF: J Mol Biol 157:105–118, 1982.
19. Lemire BD, Robinson JJ, Bradley RD, Scraba DG, Weiner JH: J Bacteriol 155:391–397, 1983.
20. Engelman DM, Henderson P, McLachlan AD, Wallace BA: Proc Natl Acad Sci USA 77:2023–2027, 1980.
21. Fitch WM: J Mol Biol 16:9–16, 1966.
22. McLachlan AD: J Mol Biol 61:409–424, 1971.
23. Manavalan P, Ponnuswamy PK: Nature 275:673–674, 1978.
24. Levitt M: Biochemistry 17:4277–4285, 1978.
25. Inouye M, Halegoua S: CRC Crit Rev Biochem 7:339–371, 1978.
26. Inouye S, Soberon X, Franceschini T, Nakamura K, Itakura K, Inouye M: Proc Natl Acad Sci USA 79:3438–3441, 1982.
27. Fillingame RH: Annu Rev Biochem 49:1079–1113, 1980.
28. Tzagoloff A, Macino G, Sebald W: Annu Rev Biochem 48:419–441, 1979.
29. Goldkorn T, Rimon G, Kempner ES, Kaback HR: Fed Proc 41:671, 1981.
30. Robinson JJ: Glycerol-3-phosphate dehydrogenase and fumarate reductase of E coli. PhD thesis, University of Alberta, 1982.